

DOI: 10.1515/amm-2016-0296

T. GIĘTKA\*#, K. CIECHACKI\*\*

## MODELING OF RAILWAY WHEELS MADE OF AUSTEMPERED DUCTILE IRON

A person is forced to travel constantly throughout its entire life. The more modern the society, the greater the pace of life, and the greater the need to be present in many places that are distant from each other. Rail transport occupies second place in this regard, after air transport. This means of transportation has many advantages, however the time of travel requires continuous improvement, in particular, to match the competition. One factor limiting the speed of travel is inter-operation between the wheels – rail kinematic pair. When rolling on a rail, a wheel is subject to wear, which unavoidably leads to its degradation. Frequent damage to both the wheel and the rail necessitates consideration of this problem. Because any changes to the rail are very expensive and time-consuming, this paper focuses on possible changes to the wheel.

This paper is of an analytical nature and is based on sources in the literature, as well as on own simulations. The objective of the paper is to indicate the advantages of using ADI (Austempered Ductile Iron) as a material for the wheel of a railway rolling stock through analysis of available scientific materials and analysis based on a conducted simulation. The application of ADI on a large scale would certainly make a large impact on the development of railway engineering, significantly reducing the costs of manufacturing the product and its future exploitation.

*Keywords:* ADI, railway wheel, modeling

### 1. Introduction

Wheel sets are the most important technical component of rail vehicles. Two types of wheel sets are distinguished according to the functions they perform and they are: driving wheel sets and rolling wheel sets. A wheel set is an axle shaft with two permanently mounted wheels [15,17]. Table 1 contains a classification of railway wheels.

TABLE 1

Classification of wagon wheel sets [6]

Classification according to:	Specification
Track gauge	<ul style="list-style-type: none"> <li>– normal-gauge wheel set</li> <li>– wide-gauge wheel set</li> <li>– narrow-gauge wheel set</li> </ul>
Diameter of wheel tread	<ul style="list-style-type: none"> <li>– normal-diameter wheels</li> <li>– small-diameter wheels</li> <li>– very small-diameter wheels</li> </ul>
Design of the connection between the axle and wheels	<ul style="list-style-type: none"> <li>– wheels permanently mounted on axle</li> <li>– slidable wheels on axle</li> </ul>

Depending on their type, wheel sets operate on tracks of different widths: normal-gauge sets on 1435 mm tracks, wide-gauge wheel sets on tracks with larger gauges, and narrow-gauge sets on gauges less than 1435 mm [6].

Band wheels (fig. 1) consist of a wheel center (this component is driven onto the axle wheel seat), band (also known as the wheel ring) and clamping ring (additional securing component).

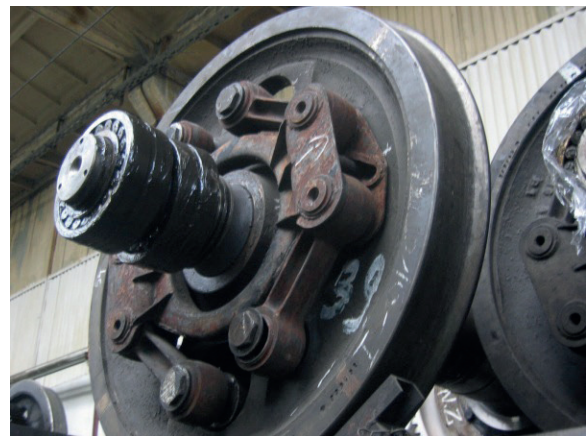


Fig. 1. Wheel with mounted band [17]

In the case of wagons with greater loads and luxury wagons, a rubber insert is installed between the wheel center and the band (fig. 2). This is meant to eliminate vibrations generated during travel and to reduce noise at the same time [7, 14].

\* UNIVERSITY OF SCIENCE AND TECHNOLOGY, DEPARTMENT OF MATERIALS SCIENCE AND ENGINEERING, FACULTY OF MECHANICAL ENGINEERING, BYDGOSZCZ, POLAND

\*\* UNIVERSITY OF SCIENCE AND TECHNOLOGY, DEPARTMENT OF MATERIALS SCIENCE AND ENGINEERING, FACULTY OF MECHANICAL ENGINEERING BYDGOSZCZ, POLAND

# Corresponding author: [tgietka@utp.edu.pl](mailto:tgietka@utp.edu.pl)

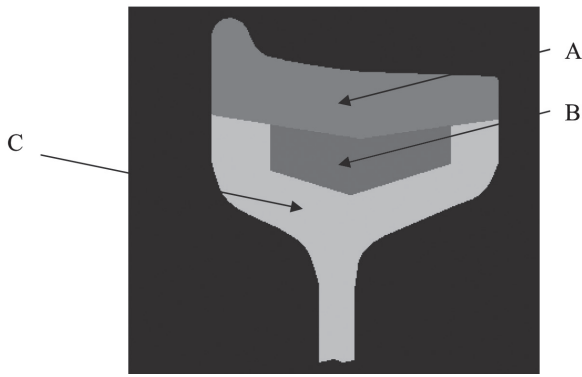


Fig. 2. Diagram of the shock-absorbing insert between the wheel center and the band: A – band, B – rubber component, C – wheel center [17]

A monoblock wheel, also known as a bandless wheel, is made as a single component, in contrast to a band wheel. The rim and hub are made as one steel component in dies on heavy presses [17].

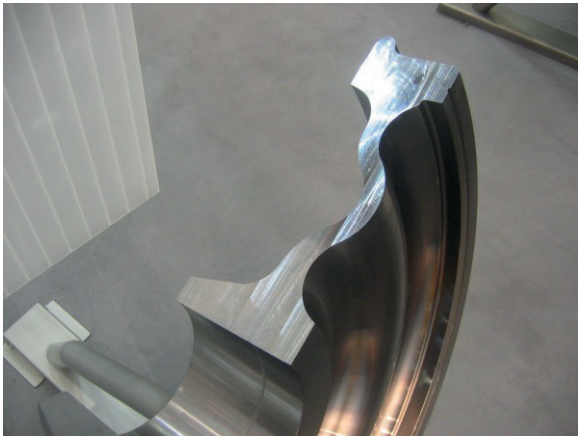


Fig. 3. Cross-section of a monoblock wheel [17]

This solution causes a significant increase of wheel exploitation costs. After final reeling – finishing work is performed, it is not possible to restore the appropriate parameters, which results in a need to uninstall and replace the wheel.

As seen in the cross-section (fig. 3), it is not possible to apply rubber inserts, and in effect, monoblock wheels have worse shock-absorbing properties than band wheels. Better safety is an advantage of such a solution, because there can be no question of clearance between components, since the wheel is a monoblock [7].

## 2. Tests conducted on ADI wheels

In the 1980's, research was conducted in Finland on ADI as an alternative material for wheels in the passenger cars of railway wagons. This research showed a 30% reduction in life cycle costs (from the start of use until scrapping). Damage that occurred on the rolling surface was the reason why continuation of ADI implementation as a material for rail wheels was abandoned [3]. At the same time, research was conducted at the Research and Technology Center of

the Deutsche Bahn AG (DB AG), where the technology of manufacturing ADI wheels for railway systems was mainly focused on – since the cause of the Finnish failure was believed to be an improper production process. Exploitation tests were performed on a rail made of steel with a pearlitic microstructure (0.8% C), designated 900 A ( $880 \text{ MPa} \leq R_m \leq 1030 \text{ MPa}$ ). Wheels were cast from ductile iron and then subjected to austenitization in a furnace with a protective atmosphere at a temperature of  $900^\circ\text{C}$ . Austempering was performed in two steps. The first step was performed immediately after austenitization in a furnace with a salt bath at a temperature of  $220^\circ\text{C}$ , and then wheels were transferred to a second furnace with a salt bath, with a temperature of  $370^\circ\text{C}$ . Wheels were left for 2 hours, after which they were after cooled in open air. To give a comparison, an identical test was performed on wheels made from R7, B6 and HH steel, with 0.5%, 0.6% and 0.7% carbon content, strength  $R_m$  amounting to 850 MPa, 1000 MPa and 1200 MPa, respectively, and  $A_5$  equal to 20%, 14% and 11%, respectively. Three normal force  $F_N$  values were accepted: 1410 N, 3935 N and 5665 N. The slip value was 3% and remained constant for all 3 normal forces. In order to compare individual material combinations, mass decrement was measured after 140,000 rotations of the inter-operating kinematic pairs. The test pair of a wheel made from ADI and rail made from 900 A steel exhibited the lowest material loss [4].

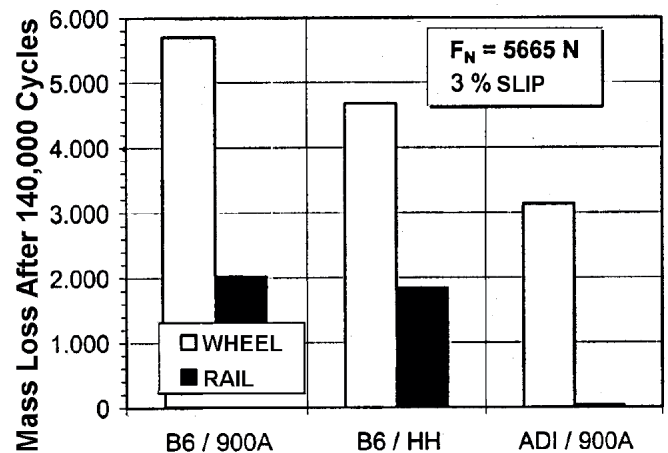


Fig. 4. Mass decrement for different wheel/rail pairs, at 3% slip and normal force  $F_N = 5665 \text{ N}$  [4]

An explanation of this phenomenon should be sought in the self-hardening capability of high-carbon austenite, a component in the microstructure of ADI. During the experiment, mass decrement and the coefficient of friction decreased, approaching a constant value. However, the wheel/rail kinematic pair (ADI/900 A steel) loaded with normal force  $F_N = 1410 \text{ N}$  did not achieve a constant wear value at 140,000 rotations. This can be explained by the fact that the accepted normal force value did not cause a self-hardening effect on the wheel's contact surface.

Figures 5a and 5b show plastically deformed areas of the surface, however no strain-induced transformation of austenite to martensite, as described in publication [1], was observed. It was observed, however, that spheroidal graphite was oriented according to the direction of loading

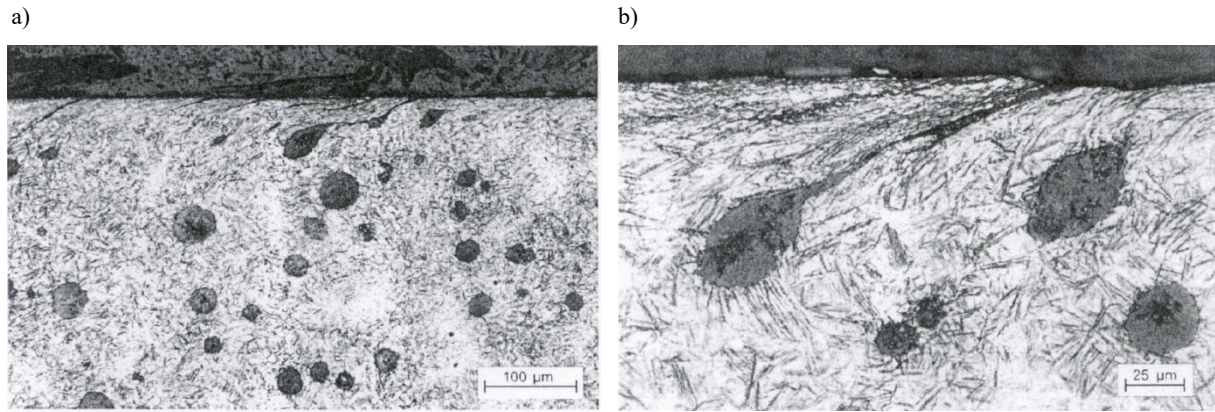


Fig. 5. Microstructure of ADI wheel surface after testing at normal force  $F_N = 5665$  N, a) magnification x100; b) magnification x250 [1]

force application. Plastic deformation below the contact surface led to the formation of micro-cracks. Micro-cracks were found in samples made of ADI, however their linear dimensions were twice as small as those found in steel wheels. Figure 5b presents the nature of present micro-cracks, which propagate from spheroidal graphite in the direction of the wheel surface.

### 3. Modeling

Using scientific papers [1÷5], related to the application of ADI for wheels of rail vehicles, as an inspiration, it was decided to conduct optimization of wheel design by comparing standardized ADI grades (according to PN-EN 1564:2012) with P70 grade steel (according to PN-EN 13262+A2:2011). Two standardized wheel models were used to conduct design optimization, and their dimensions are given in standard PN-92/K-91019. The selected wheels were: 920 185a and 920 185s ; these are the models that are most frequently used in medium-speed rail vehicles.

Modelling was conducted in the Autodesk Inventor 2011 Professional environment, which additionally included a stress analyzer based on the Ansys solver [8]. Technical drawings and models generated for optimization are presented in Figure 6.

Over the course of design analysis of the investigated material grades, the requirements that should be met by monoblock wheels in passenger and freight rail vehicles, so that they can be used in the European network, were determined. Modelled wheels were loaded with forces according to Figure 7. The direction of force application is specified in standard PN-EN 13979-1+A2:2011 [12], and their load value was accepted based on the values contained in paper [2]. Fulfillment of the aforementioned conditions is necessary before monoblock wheels can be approved for traffic. Furthermore, based on paper [2], an additional, tangential braking force  $F_h$  was applied in the place of force  $F_z$ .

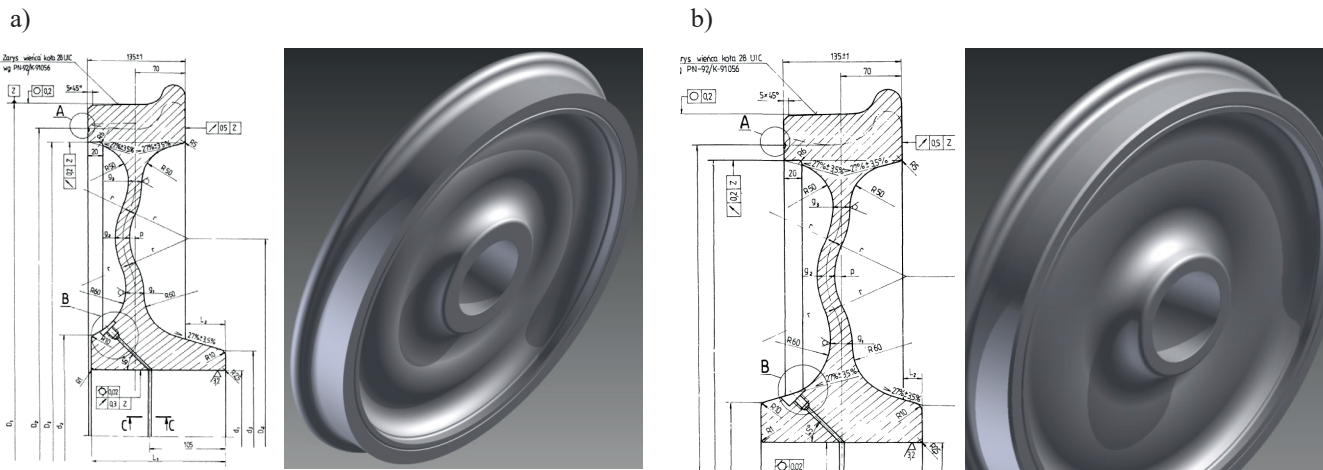


Fig. 6. Drawings and models of optimized wheels: a) 920 185a, b) 920 185s



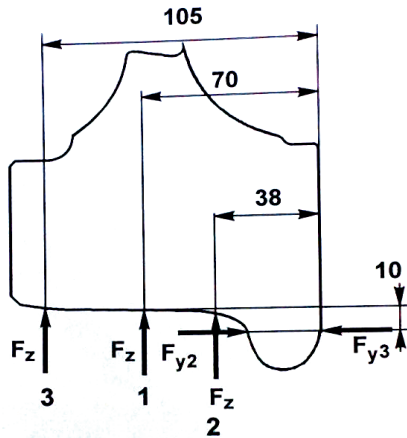


Fig. 7. Point of testing force application according to standard PN-EN 13979-1+A2:2011. Force values:  $F_z = 159.0$  kN,  $F_{y2}, F_{y3} = 62.0$  kN,  $F_h = 31.8$  kN

Material templates were made over the course of the modelling process for P70 grade steel and four ADI grades, and the values of individual properties are presented in Table 2.

The values of occurring stresses were checked when a given model and material were paired. Dimensional optimization of models was performed by comparing maximum stresses with the material's yield point. Because the wheel rim is standardized [11] and the hub must be adapted to the car axle, only the thickness of the wheel disk was changed. Reduction of this dimension lasted until maximum stresses in the model were equal to half of the tested material's yield point (a safety factor of 2 was accepted).

Ready models were transferred to the "stress analysis" environment in Autodesk Inventor software. Due to the small surface on which forces act, it was decided to apply them by means of the "point remote force" function. Bindings were defined by anchoring at the point of contact between the wheel and axle. Figure 8 presents an example of a model mesh with forces prepared in one case.

Example distributions of stresses and displacements depending on the material grade used for the monoblock wheel are presented in Figure 9.

Table 3 presents the simulation results for two wheel types (920 185a and 920 185s), with the five applied material grades accepted as their materials (according to Table 2).

As shown in Table 3, the difference for the 920 185a type wheel modelled with P70 grade steel and EN-GJS-1400-1 grade ADI amounts to 64.41 kg, and the maximum difference in disk thickness amounts to 10.9 mm. In the case of the 920 185s wheel type, values are lower and amount to 56.71 kg and 8.0 mm, respectively in terms of mass and disk thickness, to the advantage of the wheel made of ADI.

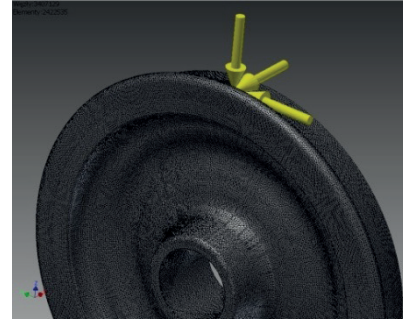


Fig. 8. Model mesh with applied forces for monoblock wheel 920 185a

#### 4. Summary

The presented simulation with the application of the Autodesk Inventor system is a preliminary tool for starting the research process. Actual load values and material behaviours can only be measured on a test or real object. Wheel parameter values obtained for the computer model should be verified by an experiment. The Autodesk Inventor modelling environment is a tool based on classical load state models, which does not account for all possibilities of material behaviour in its calculations. The analytical environment does not account for the complex state of factors occurring during exploitation of rail vehicle wheels, nor does it take all technological factors in the manufacturing process into consideration.

Such simulation is indispensable under industrial conditions, before the production process is started.

The material proposed in the paper for wheel components of rail vehicles fulfills the specified criteria in the light of the literature review and the obtained results of simulation. Based on analysis of the difference in mass of the monoblock wheel between the presented variants, it was determined that this difference amounts to 20.7% in the extreme variant, to the advantage of ADI.

Mechanical properties of the materials used in modelling [13, 16]

TABLE 2

	Material grades				
	P70 Steel	EN-GJS-800-10	EN-GJS-1050-6	EN-GJS-1200-3	EN-GJS-1400-1
Density, g/cm <sup>3</sup>	7.85	7.10	7.10	7.00	7.00
Young's modulus, GPa	210	170	168	167	165
Poisson ratio	0.30	0.27	0.27	0.27	0.27
Yield point, MPa	430	500	700	850	1100
Tensile strength, MPa	920	800	1050	1200	1400

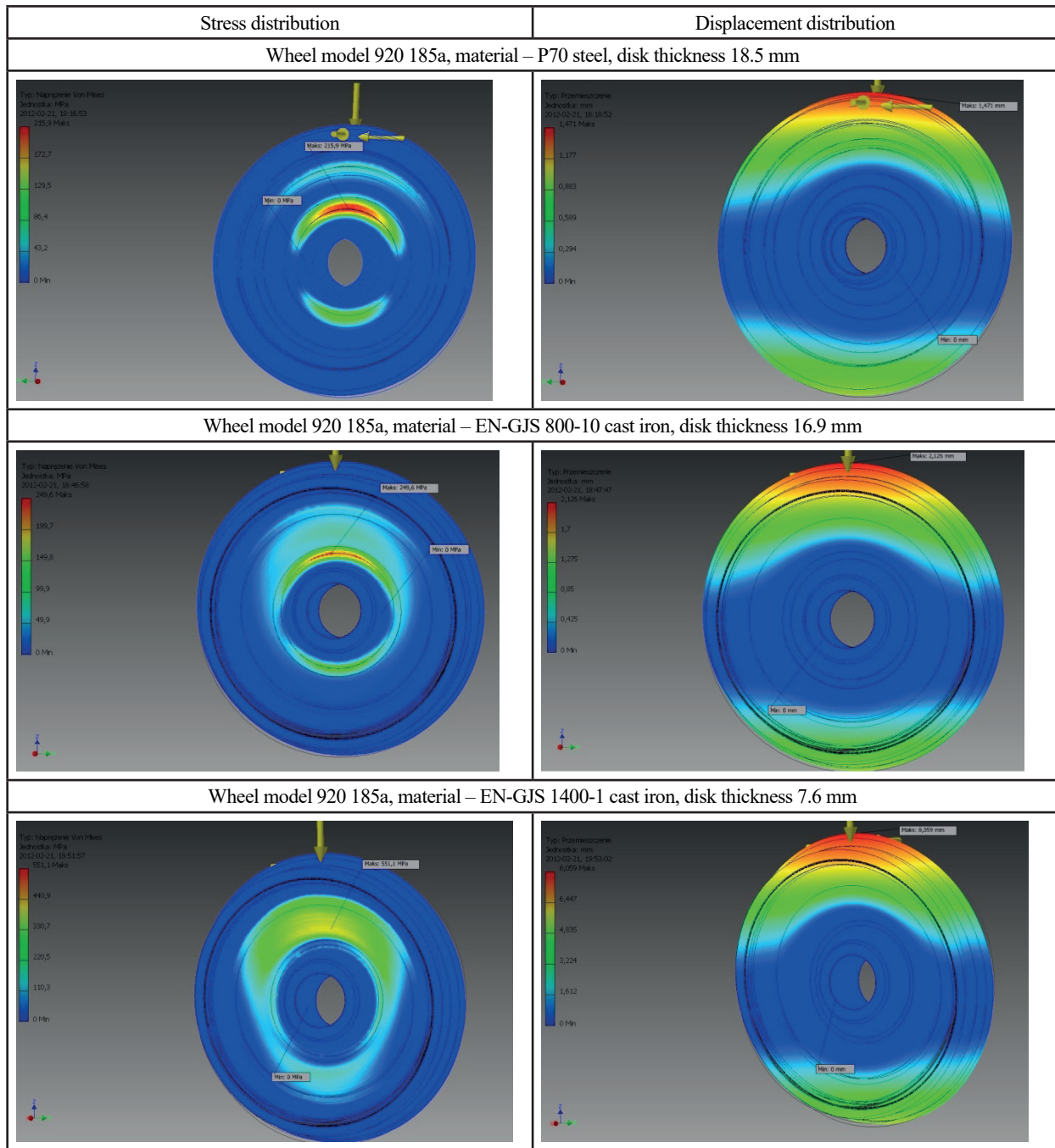


Fig. 9. Example distributions of stress and displacement [8]

TABLE 3

Presentation of collected modelling optimization results

Type of wheel	Material	Minimum disk thickness, mm	Stress, MPa	Displacement, mm	Volume, dm <sup>3</sup>	Weight, kg
920 185a	P70 Steel	18.5	215.9	1.47	43.29	339.80
	EN-GJS-800-10	16.9	249.6	2.13	42.65	302.80
	EN-GJS-1050-6	9.8	350.3	5.11	39.73	282.08
	EN-GJS-1200-3	8.8	424.3	6.10	39.32	279.15
	EN-GJS-1400-1	7.6	551.1	8.06	38.79	275.39
920 185s	P70 Steel	18.5	217.0	1.46	42.08	330.34
	EN-GJS-800-10	17.0	251.4	2.19	41.42	294.10
	EN-GJS-1050-6	13.7	350.9	3.40	39.97	283.79
	EN-GJS-1200-3	12.3	423.4	4.36	39.35	279.41
	EN-GJS-1400-1	10.5	552.4	6.16	38.54	273.63

## REFERENCES

- [1] M. N. Ahmadabadi, S. Nategh, P. Davami, Wear behavior of austempered ductile iron, *Cast Metals* **4**, 188-194 (1992).
- [2] M. Kuna, M. Springmann, K. Mädler, P. Hübner, G. Pusch, Fracture Mechanics based design of a railway wheel made of austempered ductile iron, *Engineering Fracture Mechanics* **72**, 241-253 (2005).
- [3] K. Kymenite, Railway Applications. In: Conference Group of the ADI-Seminar, Technical University Helsinki (1991).
- [4] K. Mädler, On the Suitability of ADI as an Alternative Material for (Railcar) Wheels, (2000).
- [5] S. E. Guzik, Austempered cast iron as a modern constructional material; *Material Engineering*, ISSN 0208-6247, **6**, 677-680 (2003).
- [6] R. Marczewski, J. Podemski, Technology for mechanics wagon, Publisher Transport and Communication, Warszawa (1990).
- [7] Z. Romaniszyn, Chassis rail trolley cars, Publisher Transport and Communication, Kraków (2010).
- [8] H. Minta: Design optimization of ADI rail wheels, Diploma thesis, Bydgoszcz (2012).
- [9] PN-EN 13979-1+A2:2011: Railway applications – Wheelsets and bogies – Monobloc wheels – Technical approval procedure – Part 1: Forged and rolled wheels.
- [10] PN-K-91019:1992: Wagons – Bandless wheels – Types and dimensions.
- [11] PN-EN 13715+A1:2011: Railway applications – Wheelsets and bogies – Wheels – Tread profile.
- [12] PN-EN 13979-1+A2:2011: Railway applications – Wheelsets and bogies – Monobloc wheels – Technical approval procedure – Part 1: Forged and rolled wheels.
- [13] PN-EN 13262+A2:2011: Railway applications – Wheelsets and bogies – Wheels – Product Requirements.
- [14] T. Giętka, K. Ciechacki, The aspect of application ADI Studies & Proceedings Polish Association for Knowledge Management **68**, 94-102 (2014).
- [15] B. Żółowski, M. Zółowski, Vibrations in the Assessment of Construction State, *Applied Mechanics and Materials* **617**, 136-141 (2014).
- [16] PN-EN 1564:2012: Founding–Ausferritic Spheroidal Graphite Cast Irons.
- [17] <http://www.transportszynowy.pl/zestawykolowe1.php> (23.05.2015).